Electronically delay-tuned upconversion cross-correlator for characterization of mid-infrared pulses

Huot, Laurent; Moselund, Peter Morten; Tidemand-Lichtenberg, Peter; Pedersen, Christian

Published in:
Optics Letters

Link to article, DOI:
10.1364/OL.43.002881

Publication date:
2018

Document Version
Peer reviewed version

Electronically delay-tuned upconversion cross-correlator for characterization of mid-infrared pulses

LAURENT HUOT[1,2,*], PETER MORTEN MOSELUND[1], PETER TIDEMAND-LICHTENBERG[2], AND CHRISTIAN PEDERSEN[2]

[1] NKT Photonics A/S, Blokken 84, 3460 Birkerød, Denmark
[2] DTU Fotonik, Frederiksborgvej 399, 4000 Roskilde, Denmark
[*] Corresponding author: lhu@nktphotonics.com

In this paper, a novel method for the characterization of mid-infrared pulses is presented. A cross-correlator system with no moving parts combining ultra-broadband pulsed upconversion detection with fast active electronic delay tuning was built to perform time-resolved spectral characterization of 1.6 ns mid-infrared supercontinuum pulses. Full wavelength/time spectrograms were acquired in steps of 20 ps over a range that can in theory extend to microseconds, in a matter of seconds, with 48 ps temporal resolution and 22 cm^{-1} spectral resolution in the 2700 nm to 4300 nm range. This work proves the potential of the use of electronic delay tuning instead of mechanical delay for applications like cross-correlators and laser spectroscopy where their fast precise tunability and long delay ranges are a strong asset.

OCIS codes: (040.3060) Infrared; (190.4223) Nonlinear wave mix-ing; (190.7220) Upconversion; (280.4788) Optical sensing and sensors;(320.6629) Supercontinuum generation

The use of pulsed mid-infrared (mid-IR) sources like broadband supercontinuum sources and tunable quantum cascade lasers is becoming ever more common in a variety of spectrometric optical systems for detection, identification, and quantification of chemical species. This is because the mid-IR is the wavelength region of choice for the analysis of fundamental absorption lines of many gases and vibrational spectra of many complex molecules [1–3]. It is however critical to characterize their temporal profile as well as the spectral variation within the duration of a pulse to ensure the best possible accuracy, resolution and repeatability of such measurements. Currently, there are no commercially available time-resolved spectrum analyzers in the mid-IR. Usually, mid-IR detectors are based on low band-gap semiconductor materials like indium antimonide (InSb) or mercury cadmium telluride (HgCdTe). Alternatively, micro-bolometer arrays and thermopiles are used. All these detectors suffer from inherent dark noise and require cooling to perform optimally [4]. These detection systems are usually very expensive and have slow response times that make them unsuited for the temporal characterization of pulsed lasers. Upconversion detection circumvents these difficulties of mid-IR detection by translating the mid-IR signal to the near-IR wavelength region by nonlinear parametric sum-frequency mixing in a $\chi^{(2)}$ medium [5]. The upconverted signal can thus be detected using an affordable silicon-based detector operating in the near-IR region. These detectors are known to work with much better noise and time performance than their mid-IR counterparts [6, 7] and have been used for continuous-wave upconversion spectroscopy [8]. Synchronous pulsed upconversion has been demonstrated and successfully used for imaging and spectroscopy applications [9, 10]. The addition of a tunable delay line in a pulsed upconversion setup enables the investigation of the cross-correlation of the temporal profiles of the pulses. However, the complexity of the synchronization scheme varies with the duration of the synchronized pulses and the required temporal precision. Mechanical delay-tuning [11–13] can prove very impractical for measuring ns pulses which require long delay arms. Comparatively, electronic delay tuning can prove very advantageous. It was demonstrated in [14] to perform time-resolved spectral characterization of QCL sources with a synchronization jitter of 2.5 ns and a temporal resolution of 25 ns limited by the pulse duration of the Q-switched Nd:YAG pump laser that was used for the experiment . Additionally, gain-switched diode seeded master-oscillator power amplifier (MOPA) systems have been successfully applied to electronically synchronized nonlinear frequency conversion experiments in [11] and offer laser sources with pulse durations and temporal jitter in the ps range.

In this paper, we present a novel method of performing time-resolved characterization of ns mid-IR supercontinuum pulses. In our setup, a digital delay and pulse generator provides electronic triggering, synchronization and delay tuning between the supercontinuum source and a gain-switched diode seeded MOPA. With this method, we were able to measure full wavelength/time spectrograms of the supercontinuum in a matter of seconds with a temporal resolution orders of magnitude lower than observed in previous similar work [14].

The experiment is based on the setup from [9] and is represented in Fig. 1. In this experiment, light from a mid-IR supercontinuum source is upconverted in a synchronous fashion. The externally triggered supercontinuum emits unpolarized ns pulses at 40 kHz repetition rate and its spectrum ranges from 2 µm to 4.5 µm [15]. The average power of the full supercontinuum is 80 mW and its spectrum can be considered spatially uniform (as opposed to OPG sources). The supercontinuum light is first collimated using a 50.8 mm focal length gold coated 30° off-axis parabolic mirror (OAPM 1) to a 15 mm beam diameter. It is then tightly focused inside a bulk lithium niobate ($LiNbO_3$) crystal with a 25.4 mm focal length 30° OAPM (OAPM 2). These mirrors have a uniform high reflectance in the mid-IR eliminating chromatic aberration. The crystal is undoped and of congruent composition. It is 10 mm long, has a 5 mm x 5 mm cross section and is cut for $\theta = 48°$ and $\phi = -90°$. The crystal is kept at room temperature and used within a couple of degrees from normal incidence.

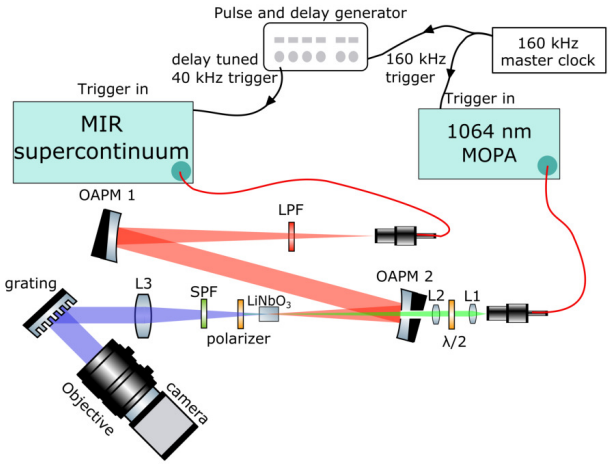

Fig. 1. Schematic representation of the experimental setup. L1 : 7.5 aspheric lens, L2 : 100 mm plano-convex lens, L3 : 60 mm achromat, OAPM 1 : 50.8 mm focal length 30° gold coated OAPM, OAPM 2 : 25.4 mm focal length 30° gold coated OAPM, LPF : 2 µm long-pass filter, SPF : 1 µm short-pass filter

The sum frequency generation is performed according to type I phase matching. We superimpose the focused supercontinuum in the nonlinear crystal with a linearly polarized 1064 nm MOPA that we will hereinafter refer to as the pump laser of the upconversion process. The direction of the polarization is adjusted using a half-wave plate to match the ordinary axis of the $LiNbO_3$ crystal. This 945 mW average power laser is based on a MOPA architecture seeded by a gain switched DFB diode from QD Laser [16]. The duration of the MOPA pulses was measured to be 40 ps FWHM with a standard autocorrelation method [17]. The short duration of the pump pulses with respect to the supercontinuum pulses make them adequate for probing the spectral content of the supercontinuum at many discrete times within the pulse. The pump light is first collimated to a 1.4 mm diameter beam with a 7.5 mm focal length aspheric lens (L1) and then focused with a 100 mm plano-convex lens (L2) so as to spatially overlap the supercontinuum focus inside the nonlinear crystal. Note that the pump beam is combined with the supercontinuum beam path by passing through a 2 mm diameter hole drilled at the top of OAPM 2 which is a simple and inexpensive method of combining the broadband IR signal with the pump beam. While the presence of the hole could cause some aberration in the system, its effects are minor due to its small size and position (rays that are not reflected due to the hole account for a very small range within the spectral acceptance bandwidth as shown subsequently). The broad spectral acceptance bandwidth of the system is achieved using non-collinear phase-matching [18].

In addition to the beams having good spatial overlap inside the nonlinear crystal, the experiment requires precise control over the temporal overlap between the pulses of both light sources. A 160 kHz master clock triggers the 1064 nm pump diode and the delay and pulse generator. This device will in turn generate one synchronized and delay-tunable trigger pulse for every four trigger pulses it receives from the 160 kHz clock signal. The newly generated 40 kHz trigger signal is used to trigger the supercontinuum source. The temporal overlap between the supercontinuum pulses and pump pulses can thus be tuned in steps of 20 ps over a range of multiple microseconds.

The pump light transmitted through the crystal is filtered out using a polarizer and a 1 µm short-pass filter and the upconverted light is collected with a 60 mm focal length achromat (L3) which collimates it onto a reflective grating blazed for 750 nm with 1200 lines/mm at an incidence angle of approximately 50°. The diffracted light is collected on a regular silicon-based camera equipped with a 50 mm focal length camera objective.

We first proceeded to characterize the timing jitter of the system. In order to do so, we characterized the jitter of each source with respect to their trigger by using a fast InGaAs photodiode placed at the position of the nonlinear crystal and a digital oscilloscope. Over the course of approximately one minute, we acquired the histogram of the time interval errors between the 50% peak height points of the rising front of the measured pulses relative to the trigger signal used to trigger both the source and the digital oscilloscope measurement. The histograms are presented in Fig. 2.

The standard deviation of the 1064 nm histogram and supercontinuum histogram are measured to be 41 ps and 44 ps respectively. These measurements are dominated by the timing jitter of the delay and pulse generator which is specified by the manufacturer to be typically 35 ps and also include the measurement jitter of the oscilloscope specified to be 4 ps. By assuming that the jitter mechanisms are independent we obtain that the jitter of the 1064 nm pump and supercontinuum sources

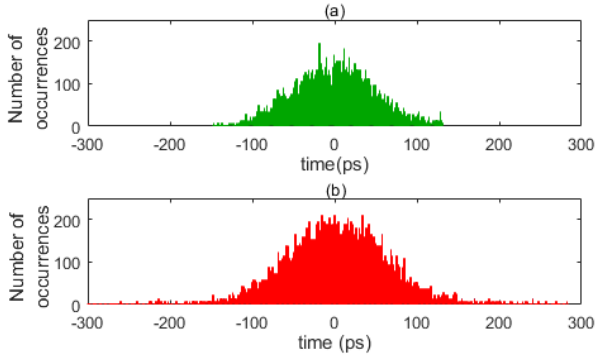

Fig. 2. (a) jitter histogram of 1064 nm MOPA pump laser with respect to a trigger pulse, (b) jitter histogram of supercontinuum with respect to a trigger pulse

are 21 ps and 26 ps respectively. The total temporal jitter in the upconversion process includes the jitter of both sources and the delay and pulse generator and is estimated to be approximately 48 ps RMS.

Next, we investigated the stability of the delay control between two pulses over a period of 30 minutes. In order to do so, both light sources were set to illuminate a single InGaAs photodiode connected to a digital oscilloscope in a way that both pulses can be visualized on the same trace. The delay between the two pulses was set to 2 ns. The delay is measured as the time difference between the moments when the rising fronts of a supercontinuum pulse and its corresponding pump pulse each reach 50% of their peak value. Each point is averaged over 100 measurements to exclude the effect of the 48 ps timing jitter. Figure 3 displays the variation of the delay between the supercontinuum and pump pulses over a period of 30 minutes measured at 30 second intervals. The average delay between the supercontinuum and pump pulses varied by approximately 45 ps. Experimentally, we observed that this is mainly due to changes in the temporal shape of the supercontinuum pulse related to temperature fluctuations of the system. This variation is negligible over the course of the <30 s measurement times presented subsequently in this paper.

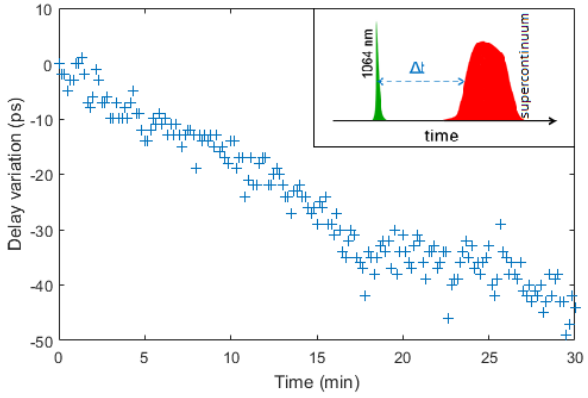

Fig. 3. Variation of the delay between the supercontinuum pulses and the 1064 nm laser pulses over the course of 30 minutes

The upconverted light is diffracted by the grating and collected on a standard silicon-based camera with an integration time of 0.4 ms. Figure 4(a,b) shows the raw camera signal obtained without (Fig. 4(a)) and with (Fig. 4(b)) a 50 µm thick polystyrene film in the beam path of the supercontinuum. The spectral features of the upconverted light appear as bright and dark pixels on the camera in a fashion similar to a traditional grating spectrometer. The wavelength scale of the spectrometer setup is calibrated against an FTIR measurement of the transmission of polystyrene by using the vibrational C-H absorption lines at 3304 nm and 3420 nm (see Fig.4(c)). We can, first of all, notice that the upconverted wavenumber band is limited by the spectral bandwidth of the upconversion process to the 2700 nm to 4300 nm wavelength range due the strong variation of the noncollinear conversion efficiency and the limited dynamic range of the detector. Approximately 540 camera pixels are illuminated and thus each pixel covers 2.6 cm^{-1}. The Figure 4(c) compares the transmission spectrum of a polystyrene film measured in our experiment with a spectrum obtained with FTIR. The plotted spectra are represented in terms of transmittance which is defined as the ratio of transmitted power over incident power. This figure is thus unaffected by the wavelength dependence of the efficiency of the upconversion process. While the FTIR spectrum was originally measured with a spectral resolution of 4 cm^{-1} the data plotted in Fig. 4(c) was modified so as to simulate a 22 cm^{-1} spectral resolution. For this spectral resolution, the upconverted spectrum (blue) and the FTIR spectrum (red) are in good agreement. This indicates that the spectral resolution of our system is approximately 22 cm^{-1}. The resolution is mainly limited by the size of entrance slit of the grating setup which is materialized by the effective overlap of the pump and IR beams in the crystal. Additionally, oscillations of the absorption lines can be observed on the transmission spectrum obtained in our experiment. These oscillations are due to interference effects arising from multiple reflections of the supercontinuum light on the surfaces of the polystyrene film.

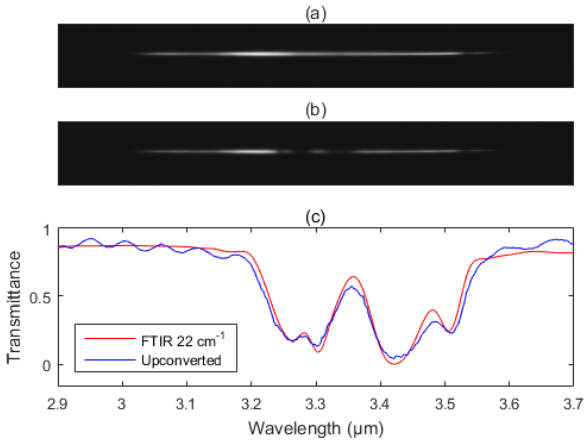

Fig. 4. (a) Raw camera image of the upconverted full supercontinuum light, (b) raw camera image of the upconverted supercontinuum light transmitted through a 50 µm polystyrene film, (c) Comparison of the transmission spectra of a 50 µm thick polystyrene film obtained with FTIR (red) and upconversion spectroscopy (blue)

Figure 5 shows the variation of the efficiency of the upconversion process with the input wavelength. This plot was obtained by tracing the ratio between the intensity of the light collected by the camera with a reference FTIR measurement of the power spectral density of the supercontinuum source. We notice that the upconversion process is more efficient at the shorter wavelengths than the longer wavelengths. This is due to the fact that the efficiency of the conversion process is strongly dependent on the overlap between the signal and the pump. In this experiment, both the signal and the pump are spatially coherent sources. Therefore, the effective overlap of their beam-waists inside the nonlinear crystal is significantly larger for the shorter collinearly upconverted wavelengths compared to the longer wavelengths which satisfy the phase matching condition for a larger incidence angle of the supercontinuum. The efficiency profile is consistent with [8] with the exception of the small dip in efficiency at 2870 nm which is due to the presence of the hole in OAPM 2.

Lastly, we performed multiple spectra acquisitions of the upconverted supercontinuum light while shifting the delay time between the trigger signals of the supercontinuum and the pump

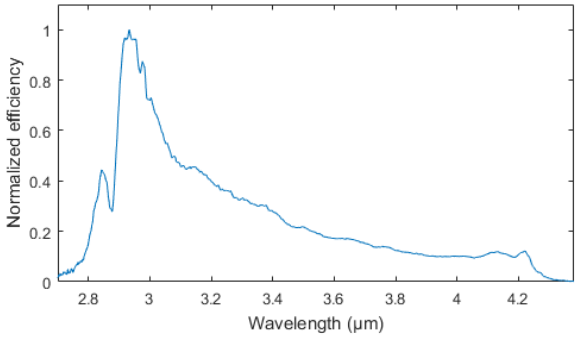

Fig. 5. Variation of the efficiency of the upconversion process as a function of input wavelength.

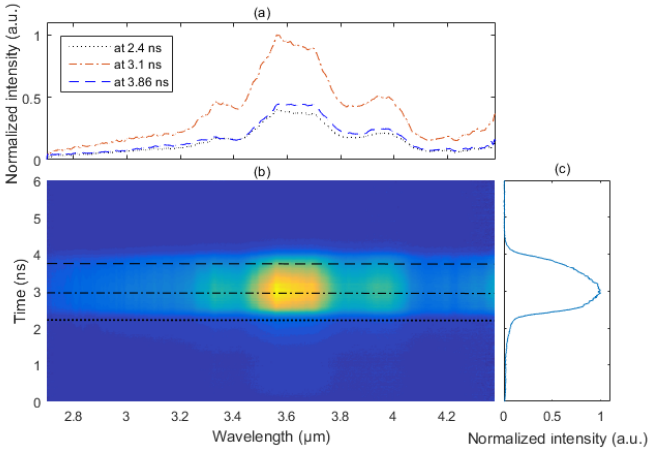

Fig. 6. (a) Comparison of the spectra at 2.4 ns (black dotted), at 3.1 ns (red dot/dash) and at 3.86 ns (blue dashed), (b) spectrogram of the supercontinuum pulses, (c) Temporal profile of the supercontinuum pulse.

by 20 ps for each measurement in order to obtain a full wavelength/time spectrogram. Spectra were thus acquired for 300 delay values spread over 6 ns. The camera integration time for one full spectrum was 0.4 ms, and each spectrum was averaged over 50 consecutive measurements. Therefore, each spectrum represents the average spectrum of 800 consecutive supercontinuum pulses, thus removing the strong pulse to pulse fluctuations of the ns supercontinuum source [15]. Each spectrum was also corrected for the wavelength dependence of the efficiency of the upconversion process (Fig. 5). The electronic delay line allowed the entire measurement process to be automated and the acquisition of the full spectrogram took less than 30 seconds. Figure 6 shows the variation of the upconverted wavelength range of the supercontinuum pulses as a function of time. We first note that the spectrum is mostly uniform along the duration of a pulse and that these pulses are 1.6 ns FWHM. At a given wavelength, the upconverted signal as a function of delay is the temporal cross-correlation of the temporal profiles of the IR signal and the pump. Since the pulse lengths (Fig. 6(c)) of the supercontinuum in this experiment are significantly longer than the 40 ps FWHM pump pulses, the cross-correlation preserves the temporal profile of the IR signal with good fidelity and thus does not require any deconvolution processing.

In conclusion, we have demonstrated a system capable of time-resolved spectral characterization of broadband mid-IR pulses based on electronically controlled delay tuning. The system yielded full spectrograms of ns supercontinuum in 20 ps steps over a delay range of 6 ns, with 48 ps temporal resolution and approximately 22 cm^{-1} spectral resolution in the 2700 nm to 4300 nm wavelength range in less than 30 s. The digital delay and pulse generator allows for fully automated active delay tuning of the IR pulse with respect to the pump pulse with a precision of tens of ps over delays that can be as long as multiple μs without the need for mechanical delay lines. This system could easily be adapted to perform time-resolved spectral characterization of QCL and Q-switched lasers. It could also further be improved to perform single pulse measurements in order to study pulse to pulse noise dynamics. The active electronic synchronization scheme is extremely versatile as it can be used to simultaneously control and automate any number of processes like the emission of optical pulses and time gated detection among others, and we believe that it could be a powerful tool for frequency mixing applications, laser spectroscopy, and range-resolved sensing.

FUNDING INFORMATION

The Mid-TECH project has received funding from the European Union's Horizon 2020 research and innovation programme under Grant Agreement No. 642661.

REFERENCES

1. R. F. Curl, F. Capasso, C. Gmachl, A. A. Kosterev, B. McManus, R. Lewicki, M. Pusharsky, G. Wysocki, and F. K. Tittel, Chem. Phys. Lett. **487**, 1 (2010).
2. A. B. Seddon, T. M. Benson, S. Sujecki, N. Abdel-Moneim, Z. Tang, D. Furniss, L. Sojka, N. S. ad Nallala Jayakrupakar, G. R. Lloyd, I. Lindsay, J. Ward, M. Farries, P. M. Moselund, B. Napier, S. Lamrini, U. Møller, I. Kubat, C. R. Petersen, and O. Bang, ProcSPIE **9703**, 970302 (2016).
3. J. Kilgus, K. Duswald, G. Langer, and M. Brandstetter, Appl. Spectrosc. **72**, 634 (2018). PMID: 29164925.
4. A. Rogalski, *Infrared Detectors* (CRC Press, 2011).
5. J. S. Dam, P. Tidemand-Lichtenberg, and C. Pedersen, Nat Photonics **6**, 788 (2012).
6. L. Høgstedt, J. S. Dam, A.-L. Sahlberg, Z. Li, M. Aldén, C. Pedersen, and P. Tidemand-Lichtenberg, Opt. Lett. **39**, 5321 (2014).
7. L. Meng, A. Fix, M. Wirth, L. Høgstedt, P. Tidemand-Lichtenberg, C. Pedersen, and P. J. Rodrigo, Opt. Express **26**, 3850 (2018).
8. S. Wolf, J. Kiessling, M. Kunz, G. Popko, K. Buse, and F. Kühnemann, Opt. Express **25**, 14504 (2017).
9. L. Huot, P. M. Moselund, L. Leick, P. Tidemand-Lichtenberg, and C. Pedersen, ProcSPIE **10088**, 100880J (2017).
10. S. Dupont, P. M. Moselund, L. Leick, J. Ramsay, and S. R. Keiding, J. Opt. Soc. Am. B **30**, 2570 (2013).
11. L. Abrardi and T. Feurer, ProcSPIE **8237**, 82373W (2012).
12. J. Ramsay, S. Dupont, M. Johansen, L. Rishøj, K. Rottwitt, P. M. Moselund, and S. R. Keiding, Opt. Express **21**, 10764 (2013).
13. S. Wolf, T. Trendle, J. Kiessling, J. Herbst, K. Buse, and F. Kühnemann, Opt. Express **25**, 24459 (2017).
14. J.-M. Melkonian, M. Raybaut, A. Godard, J. Petit, and M. Lefebvre, ProcSPIE **8546**, 854607 (2012).
15. Opt. Fiber Technol. **18**, 349 (2012).
16. S. Kanzelmeyer, H. Sayinc, T. Theeg, M. Frede, J. Neumann, and D. Kracht, Opt. Express **19**, 1854 (2011).
17. J. A. Armstrong, Appl. Phys. Lett. **10**, 16 (1967).
18. P. Tidemand-Lichtenberg, J. S. Dam, H. V. Andersen, L. Høgstedt, and C. Pedersen, J. Opt. Soc. Am. B **33**, D28 (2016).

FULL REFERENCES

1. R. F. Curl, F. Capasso, C. Gmachl, A. A. Kosterev, B. McManus, R. Lewicki, M. Pusharsky, G. Wysocki, and F. K. Tittel, "Quantum cascade lasers in chemical physics," Chem. Phys. Lett. **487**, 1 – 18 (2010).
2. A. B. Seddon, T. M. Benson, S. Sujecki, N. Abdel-Moneim, Z. Tang, D. Furniss, L. Sojka, N. S. ad Nallala Jayakrupakar, G. R. Lloyd, I. Lindsay, J. Ward, M. Farries, P. M. Moselund, B. Napier, S. Lamrini, U. Møller, I. Kubat, C. R. Petersen, and O. Bang, "Towards the mid-infrared optical biopsy," ProcSPIE **9703**, 970302 (2016).
3. J. Kilgus, K. Duswald, G. Langer, and M. Brandstetter, "Mid-infrared standoff spectroscopy using a supercontinuum laser with compact fabry–pérot filter spectrometers," Appl. Spectrosc. **72**, 634–642 (2018). PMID: 29164925.
4. A. Rogalski, *Infrared Detectors* (CRC Press, 2011).
5. J. S. Dam, P. Tidemand-Lichtenberg, and C. Pedersen, "Room temperature mid-ir single photon spectral imaging," Nat Photonics **6**, 788–793 (2012).
6. L. Høgstedt, J. S. Dam, A.-L. Sahlberg, Z. Li, M. Aldén, C. Pedersen, and P. Tidemand-Lichtenberg, "Low-noise mid-ir upconversion detector for improved ir-degenerate four-wave mixing gas sensing," Opt. Lett. **39**, 5321–5324 (2014).
7. L. Meng, A. Fix, M. Wirth, L. Høgstedt, P. Tidemand-Lichtenberg, C. Pedersen, and P. J. Rodrigo, "Upconversion detector for range-resolved dial measurement of atmospheric ch4," Opt. Express **26**, 3850–3860 (2018).
8. S. Wolf, J. Kiessling, M. Kunz, G. Popko, K. Buse, and F. Kühnemann, "Upconversion-enabled array spectrometer for the mid-infrared, featuring kilohertz spectra acquisition rates," Opt. Express **25**, 14504–14515 (2017).
9. L. Huot, P. M. Moselund, L. Leick, P. Tidemand-Lichtenberg, and C. Pedersen, "Broadband upconversion imaging around 4 μm using an all-fiber supercontinuum source," ProcSPIE **10088**, 100880J (2017).
10. S. Dupont, P. M. Moselund, L. Leick, J. Ramsay, and S. R. Keiding, "Up-conversion of a megahertz mid-ir supercontinuum," J. Opt. Soc. Am. B **30**, 2570–2575 (2013).
11. L. Abrardi and T. Feurer, "Electronic synchronization of gain-switched laser diode seeded fiber amplifiers," ProcSPIE **8237**, 82373W (2012).
12. J. Ramsay, S. Dupont, M. Johansen, L. Rishøj, K. Rottwitt, P. M. Moselund, and S. R. Keiding, "Generation of infrared supercontinuum radiation: spatial mode dispersion and higher-order mode propagation in zblan step-index fibers," Opt. Express **21**, 10764–10771 (2013).
13. S. Wolf, T. Trendle, J. Kiessling, J. Herbst, K. Buse, and F. Kühnemann, "Self-gated mid-infrared short pulse upconversion detection for gas sensing," Opt. Express **25**, 24459–24468 (2017).
14. J.-M. Melkonian, M. Raybaut, A. Godard, J. Petit, and M. Lefebvre, "Time-resolved spectral characterization of a pulsed external-cavity quantum cascade laser," ProcSPIE **8546**, 854607 (2012).
15. "Modulation instability initiated high power all-fiber supercontinuum lasers and their applications," Opt. Fiber Technol. **18**, 349 – 374 (2012).
16. S. Kanzelmeyer, H. Sayinc, T. Theeg, M. Frede, J. Neumann, and D. Kracht, "All-fiber based amplification of 40 ps pulses from a gain-switched laser diode," Opt. Express **19**, 1854–1859 (2011).
17. J. A. Armstrong, "Measurement of picosecond laser pulse widths," Appl. Phys. Lett. **10**, 16–18 (1967).
18. P. Tidemand-Lichtenberg, J. S. Dam, H. V. Andersen, L. Høgstedt, and C. Pedersen, "Mid-infrared upconversion spectroscopy," J. Opt. Soc. Am. B **33**, D28–D35 (2016).